Supplementary Information for "Timing of Martian Core Formation from Models of Hf–W Evolution Coupled with *N*-body Simulations"

Contents of this File

Text S1

Figures S1–S3

Tables S1–S3

Supplementary References

Text S1

The Martian mantle (i.e., Shergottite source) $f^{\mathrm{Hf/W}}$ used in this study (2.0 ± 0.4, Table S1) is different than the value (~3.4) reported by Foley et al. (2005) and Dauphas & Pourmand (2011) and used in some earlier models of Martian Hf–W evolution (e.g., Morishima et al., 2013). We use the $f^{\mathrm{Hf/W}}$ of Kleine & Walker (2017), which is the most recent published estimate, and which agrees with the value reported by Jacobsen (2005). The difference between these values is not due to discrepancies in Martian meteorite measurements; in fact, the Kleine & Walker (2017) value derives from the bulk $(Hf/W)_{Mars}$ of Dauphas & Pourmand (2011). Rather, the difference arises from the $\left(^{180}Hf/^{184}W\right)_{CHUR}$ value used (Equation 2). Dauphas & Pourmand (2011) use a CHUR composition defined as a Mars-like mixture of meteoritic sources (Lodders & Fegley, 1997), rather than a CI-like value as in Kleine & Walker (2017) or Nimmo & Kleine (2007). Since the distinction is in a constant reference ratio, the actual implied timescale of accretion is identical for either $f^{\mathrm{Hf/W}}$. A body that differentiated at some time after CAI will reach a fixed final $\varepsilon_{182\mathrm{W}}$ regardless of which $f^{\mathrm{Hf/W}}$ is used because the implied initial $\left(^{182}W/^{180}W\right)_{mantle}$ is the same in each case.

Figure S1

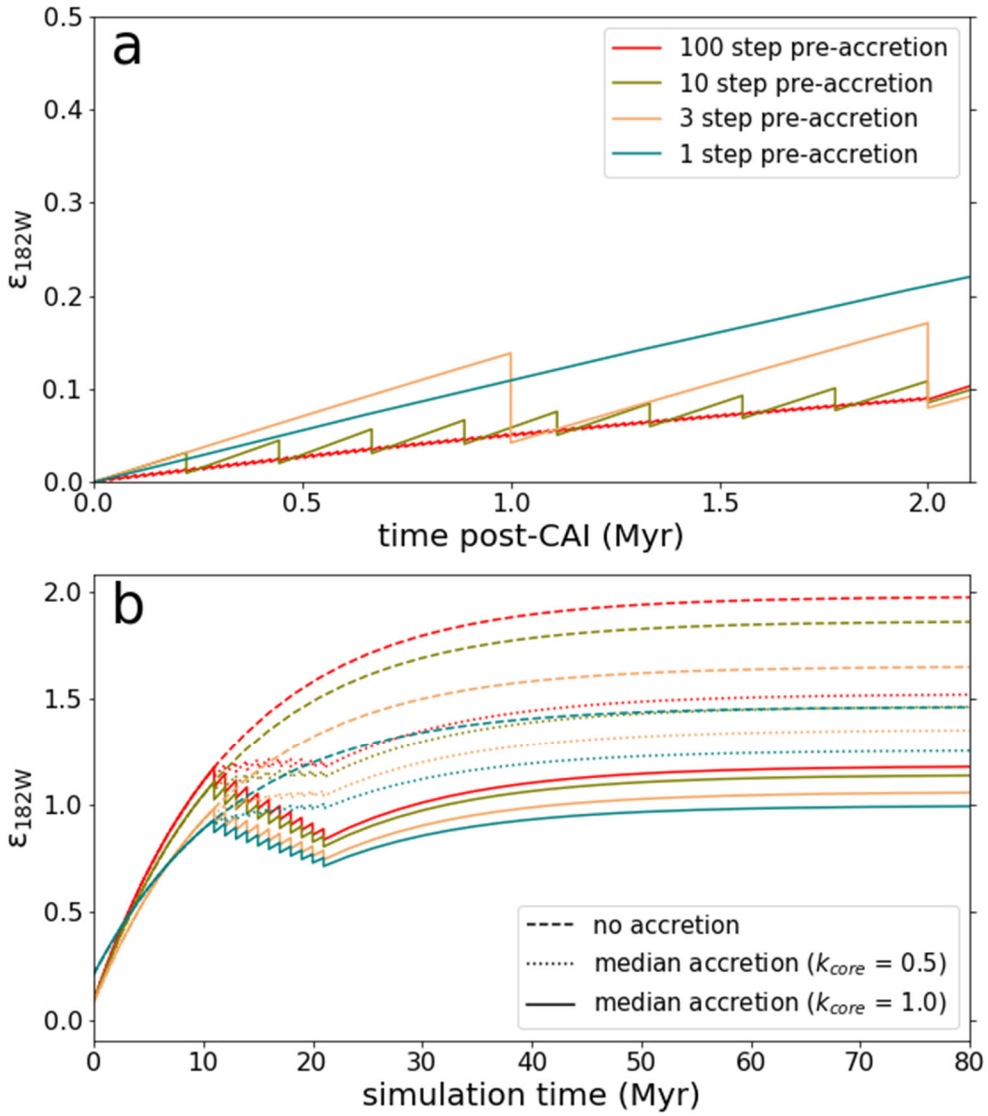

Effect of "pre-accretion" (i.e., oligarchic growth before the *N*-body simulation begins) shown by the evolution of a single embryo with variable pre-accretion history. Pre-accretion (**a**) consists of homogenous growth steps (k_{core} = 1.0) evenly distributed over the 2 Myr period between CAI condensation and the start of the *N*-body simulation. The effect of increasing the number of steps becomes negligible beyond 100 steps. During the simulation (**b**), the embryo experiences either no accretion (dashed curves) or a synthetic accretion history based on the median of the Mars analogs (11 planetesimal impactors, 95% mass reached 18 Myr after simulation start; Table S2) with k_{core} = 0.5 (dotted curves) or k_{core} = 1.0 (solid curves). The maximum possible effect of pre-accretion is ~0.5ε, and the effect is substantially smaller for most analogs.

Figure S2

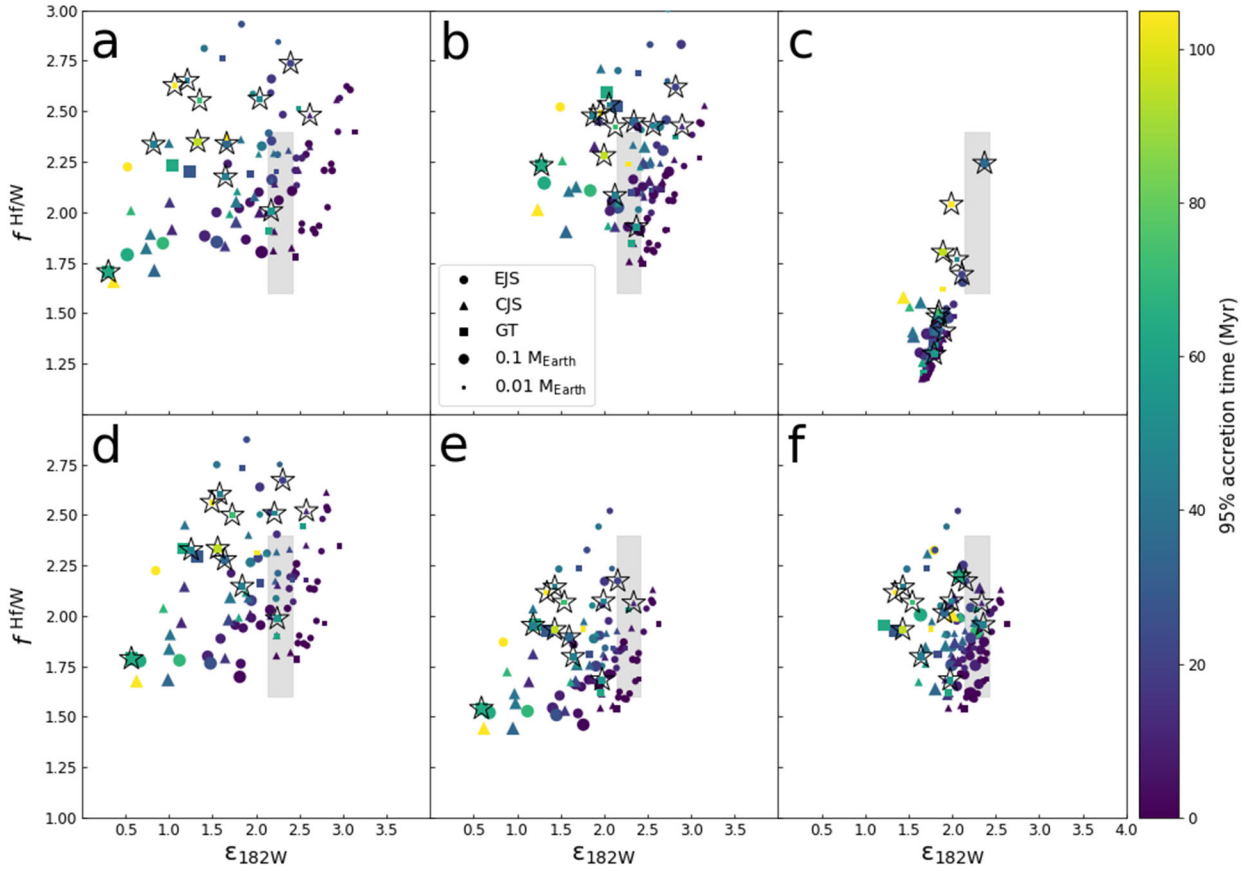

Alternate version of Figure 5 with relaxed parameter constraints. Symbol color indicates 95% accretion times, and symbol size is proportional to mass. Shaded grey region indicates the uncertainty range of measured Martian Shergotty-source values (Table S1). **a.** fO_2 = IW–1.22, 2.7 wt% S, k_{mantle} = 1.0, k_{core} = 1.0, P_{frac} = 0.5. **b.** fO_2 = IW–1.2, 5 wt% S, k_{mantle} = 0.5, k_{core} = 0.3, P_{frac} = 0.6. **c.** Initial fO_2 of IW–4 inside 1.5 AU, IW–1 outside 1.5 AU, 3.5 wt% S, k_{mantle} = 0.4, k_{core} = 0.2, P_{frac} = 0.3. **d.** fO_2 = IW–1.22, 3.5 wt% S, k_{mantle} = 0.4, k_{core} = 0.85, P_{frac} = 0.6, 4 Myr between CAI condensation and simulation start. **e.** fO_2 = IW–1.22, 3.5 wt% S, k_{mantle} = 0.4, k_{core} = 0.85, P_{frac} = 0.6, ΔT = 300 K. **f.** Same as **e** but with k_{core} = 0 (direct core merging) for embryo–embryo impacts.

Figure S3

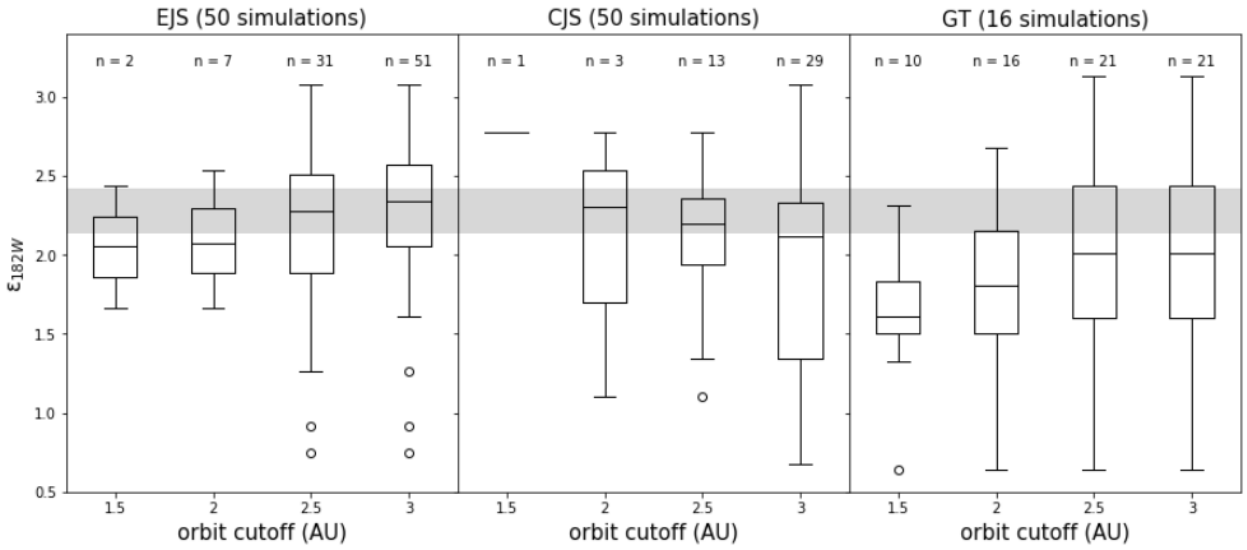

Orbital distribution of final analog ^{182}W anomalies under "reference case" model conditions (Figure 5a; fO_2 = IW–1.22, 3.5 wt% S, k_{mantle} = 0.4, k_{core} = 0.85, P_{frac} = 0.4). The shaded band indicates the measured Martian value with uncertainty (Table S3). As in Figure 2 of the main text, there does not appear to be a strong relationship between a body's final orbit and its final ε_{182W}. This implies that accretion history is independent of final analog orbit. For example, if analogs with more distant orbits took substantially longer to accrete, there would be a negative correlation between orbit cutoff and ε_{182W}.

Table S1

element	abundance (wt%)	geochemistry
Fe	43.78	partitioned (D_{Fe})
Si	25.10	perfectly lithophile
Mg	22.38	perfectly lithophile
Ni	2.56	partitioned (D_{Fe})
Ca	2.61	perfectly lithophile
Al	2.40	perfectly lithophile
Na	1.16	perfectly lithophile
Hf	3.06×10^{-5}	perfectly lithophile
W	2.75×10^{-5}	partitioned (D_W)
S	variable (1.0–5.0)	perfectly siderophile

Bulk Mars composition used in this study. Compositions are based on a CI chondrite with the highly volatile elements removed and the refractory elements enhanced by a factor of 1.22 (Palme & O'Neill, 2014). Bulk S was varied in the range 1–5 wt% and composition was renormalized to 100 wt% for each analog.

Table S2

analog ID	mass (M_{Earth})	ecc.	SMA (AU)	prov. (AU)	t_{50} (Myr)	t_{95} (Myr)	planetesimals accreted	embryos accreted	$f^{Hf/W}$	ε_{182W}
EJS3:65	0.0593	0.229	2.33	2.75	0	8.66	9	0	1.89	2.12
EJS7:55	0.1060	0.148	2.24	1.95	0.19	42.86	25	1	2.15	2.05
EJS8:63	0.1150	0.149	2.85	2.39	0.25	2.54	17	1	1.96	2.30
EJS9:52	0.0489	0.348	1.73	1.83	0	48.50	11	0	2.20	1.87
EJS9:64	0.0521	0.159	2.94	2.68	0	0	2	0	1.65	2.21
EJS10:67	0.0670	0.209	2.68	2.89	0	0.10	13	0	2.02	2.34
EJS11:61	0.1080	0.135	1.91	2.17	5.15	5.15	10	1	1.90	1.77
EJS16:51	0.0471	0.555	2.27	1.83	0	6.21	10	0	2.18	2.60
EJS16:63	0.0549	0.098	2.53	2.54	0	42.68	6	0	1.84	2.01
EJS18:49	0.1770	0.020	2.03	1.77	1.36	69.40	13	3	1.82	1.05
EJS18:53	0.0608	0.005	1.00	1.66	0	40.82	22	0	2.44	1.47
EJS21:53	0.1470	0.099	2.39	2.26	0.19	10.78	9	2	1.81	1.46
EJS22:52	0.0499	0.174	2.85	1.88	0	0.63	12	0	2.23	2.68
EJS23:62	0.0497	0.261	2.22	2.51	0	0.00	2	0	1.66	2.35
EJS23:65	0.0613	0.101	2.57	2.69	0	3.54	10	0	1.96	2.30
EJS24:65	0.0684	0.290	2.32	2.57	0	14.10	17	0	2.15	2.14
EJS25:56	0.0555	0.066	2.24	2.05	0	1.30	14	0	2.23	2.72
EJS26:54	0.1080	0.106	1.55	1.75	2.81	35.04	29	1	2.16	1.69
EJS26:60	0.0485	0.061	2.52	2.35	0	0	3	0	1.73	2.43
EJS26:61	0.0486	0.096	2.11	2.38	0	0	2	0	1.67	2.21
EJS26:64	0.0591	0.129	2.55	2.61	0	10.07	9	0	1.94	2.26
EJS26:65	0.0593	0.144	2.14	2.75	0	0.14	8	0	1.89	2.44
EJS27:67	0.0690	0.051	2.07	2.79	0	34.30	16	0	2.06	2.01
EJS28:63	0.1010	0.072	2.24	2.17	3.02	4.90	7	1	1.89	1.88
EJS28:64	0.1790	0.256	2.39	2.39	0.17	26.46	22	2	1.81	1.61
EJS29:51	0.0994	0.036	2.02	1.66	0.69	21.84	22	1	2.16	2.13
EJS29:66	0.1710	0.033	2.64	2.86	0.12	1.29	10	2	1.74	2.04
EJS30:61	0.0546	0.046	2.29	2.37	0	35.28	10	0	1.95	2.05
EJS31:37	0.0387	0.133	2.05	1.28	0	31.55	11	0	2.41	2.12
EJS31:64	0.0591	0.169	2.56	2.55	0	12.98	9	0	1.94	2.21
EJS33:42	0.0839	0.141	2.54	1.59	8.00	8.00	13	1	2.08	1.67
EJS34:31	0.0949	0.174	2.61	1.08	0.03	16.72	40	1	2.44	2.16
EJS35:50	0.1350	0.230	2.25	1.66	0.05	19.88	24	2	2.05	2.16
EJS35:58	0.0585	0.442	2.43	2.09	0	17.76	15	0	2.22	2.04
EJS36:35	0.0487	0.411	2.57	1.25	0	40.27	22	0	2.66	1.96
EJS37:62	0.1060	0.355	2.80	2.44	0.03	1.98	10	1	1.90	2.16
EJS38:67	0.1020	0.018	2.67	2.35	0	4.28	9	1	1.94	1.96
EJS39:53	0.0983	0.137	2.25	1.51	11.29	189.28	19	1	2.11	0.65
EJS39:58	0.0494	0.118	2.22	2.19	0	0	18	0	1.91	2.48
EJS40:61	0.0516	0.196	2.28	2.41	0	12.06	5	0	1.82	2.19
EJS40:68	0.0583	0.133	2.70	3.04	0	0.02	3	0	1.65	2.31

analog ID	mass (M_{Earth})	ecc.	SMA (AU)	prov. (AU)	t_{50} (Myr)	t_{95} (Myr)	planetesimals accreted	embryos accreted	$f^{Hf/W}$	ε_{182W}
EJS42:68	0.0623	0.334	1.15	3.00	0	0.59	7	0	1.81	2.17
EJS43:67	0.0629	0.050	2.89	2.94	0	1.11	9	0	1.90	2.51
EJS44:27	0.0469	0.160	2.64	0.93	0	17.89	24	0	2.75	2.12
EJS44:57	0.0645	0.123	1.54	2.01	0	20.93	22	0	2.38	2.26
EJS44:69	0.1150	0.203	2.44	2.84	0	9.62	10	1	1.85	1.54
EJS46:65	0.0533	0.274	2.72	2.75	0	0	2	0	1.64	2.32
EJS48:45	0.0537	0.274	1.97	1.46	0	24.52	21	0	2.54	1.83
EJS48:68	0.1100	0.151	2.99	2.74	0	4.75	2	1	1.75	1.82
EJS50:45	0.1990	0.696	2.47	1.39	19.62	63.81	32	1	1.78	0.64
EJS50:55	0.0485	0.863	2.36	2.01	0	4.05	8	0	2.04	2.56
CJS4:24	0.1310	0.326	2.43	1.51	5.07	16.76	35	2	2.06	1.14
CJS5:72	0.0642	0.448	2.89	3.48	0	0	3	0	1.61	2.00
CJS7:58	0.0534	0.203	2.84	2.22	0	6.84	10	0	2.07	2.41
CJS7:65	0.0603	0.555	1.54	2.68	0	29.90	9	0	1.93	2.04
CJS8:57	0.1040	0.212	2.23	2.11	0.68	34.18	15	1	2.00	1.99
CJS8:66	0.0616	0.101	2.53	2.82	0	9.89	9	0	1.91	2.07
CJS8:70	0.0652	0.110	2.16	3.20	0	14.21	7	0	1.78	1.97
CJS9:51	0.1620	0.251	2.82	1.92	0.01	22.32	35	2	1.97	1.88
CJS10:71	0.0647	0.023	2.61	3.33	0	3.67	5	0	1.70	2.03
CJS11:53	0.0508	0.122	1.47	1.97	0	11.94	12	0	2.22	2.44
CJS11:58	0.1010	0.305	2.66	1.98	24.82	69.62	11	1	1.96	0.70
CJS11:71	0.0627	0.135	2.87	3.34	0	0.00	3	0	1.62	2.17
CJS12:45	0.1020	0.192	2.65	1.40	12.50	40.68	34	1	2.30	1.14
CJS12:66	0.0707	0.495	2.10	2.71	0	40.10	18	0	2.15	1.81
CJS13:71	0.1260	0.078	2.86	3.10	3.17	16.74	9	1	1.78	1.67
CJS16:67	0.0660	0.664	2.48	2.87	0.00	2.73	13	0	1.99	2.31
CJS18:50	0.1580	0.075	2.03	1.81	0.10	41.77	45	2	2.06	1.88
CJS18:63	0.0609	0.244	2.34	2.55	0	36.04	12	0	2.06	2.09
CJS19:68	0.1690	0.034	1.94	2.22	8.84	42.00	20	2	1.86	0.88
CJS21:60	0.0555	0.224	2.29	2.29	0	49.75	10	0	2.04	1.94
CJS23:72	0.0733	0.331	2.27	3.30	0	55.45	12	0	1.90	1.73
CJS28:53	0.0538	0.147	2.88	1.94	0	3.46	15	0	2.30	2.72
CJS30:76	0.1970	0.108	2.67	3.06	12.01	35.20	24	2	1.75	0.96
CJS31:59	0.0545	0.316	2.31	2.25	0	24.10	10	0	2.06	2.22
CJS32:65	0.1280	0.217	2.98	2.65	0.31	7.76	23	1	1.95	2.06
CJS37:40	0.1400	0.382	2.77	1.58	8.47	12.00	21	2	1.94	1.15
CJS40:69	0.1940	0.214	2.88	2.42	19.60	175.43	16	2	1.72	0.50
CJS48:76	0.0791	0.459	2.79	3.82	0	62.47	11	0	1.80	1.65
CJS49:73	0.1470	0.137	2.83	2.88	18.96	40.88	26	1	1.88	0.91
GT1:38	0.0543	0.115	2.14	2.81	0	62.64	6	0	1.69	1.96
GT2:26	0.0567	0.030	1.46	1.89	0	55.91	6	0	1.78	2.00
GT2:38	0.0518	0.160	2.17	2.86	0	0	5	0	1.57	2.18
GT5:40	0.0617	0.117	1.43	2.76	0	44.47	7	0	1.95	1.61

analog ID	mass (M_{Earth})	ecc.	SMA (AU)	prov. (AU)	t_{50} (Myr)	t_{95} (Myr)	planetesimals accreted	embryos accreted	$f^{Hf/W}$	ε_{182W}
GT6:10	0.1634	0.027	1.01	1.45	0.35	28.79	63	0	2.22	1.41
GT7:30	0.0697	0.043	1.41	2.17	0	94.99	13	0	2.14	1.39
GT8:30	0.0620	0.287	1.68	2.20	0	24.32	18	0	1.96	1.86
GT9:43	0.0332	0.073	1.89	1.82	0	57.59	15	0	2.22	2.31
GT9:74	0.0359	0.045	1.47	2.53	0	110.90	5	0	2.34	1.16
GT10:18	0.1586	0.048	1.26	1.45	0.82	63.91	61	1	2.26	1.23
GT10:41	0.0283	0.195	2.01	1.67	0	11.35	3	0	1.91	2.22
GT10:43	0.0310	0.466	2.18	1.80	0	0.01	4	0	2.10	2.78
GT11:33	0.0257	0.235	2.06	1.45	0	0.00	1	0	1.67	2.37
GT11:37	0.0624	0.042	1.52	1.72	0.06	44.89	9	1	2.20	0.95
GT12:24	0.0413	0.111	1.79	1.47	0	26.47	10	0	2.50	1.66
GT12:33	0.0283	0.251	1.88	1.57	0	24.02	3	0	1.91	2.04
GT14:15	0.1741	0.069	1.49	1.53	43.99	63.80	24	2	1.78	0.45
GT14:69	0.0307	0.030	1.74	2.49	0	117.00	2	0	2.08	1.62
GT15:45	0.0338	0.033	1.41	1.85	0	72.49	7	0	2.26	1.39
GT16:50	0.0339	0.082	1.48	2.01	0	48.89	8	0	2.26	1.96
GT16:52	0.0364	0.073	1.45	1.98	0	45.03	16	0	2.37	1.29

Analog properties. Mass, eccentricity (ecc.), semi-major axis (SMA), and Hf–W values are given at the end of the *N*-body simulation. Provenance (prov.) is the mass-weighted average of the initial semi-major axes of the analog's building blocks. Times are given in simulation time (starting 2 Myr after CAI formation), with t_{50} and t_{95} being the times at which the analog reached 50% and 95% of its final mass, respectively (a value of 0 indicates that the threshold was reached before the start of the simulation). Counts of accreted bodies only include planetesimals and embryos that impacted the analog itself, and do not include any which had previously impacted those impactors. Hf–W evolution was calculated with a parameter combination that closely matches the distribution of analogs' Hf/W to the $f^{Hf/W}$ value of the Martian mantle (Figure 5c; fO_2 = IW–1.15, 3.5 wt% S, k_{mantle} = 1.0, k_{core} = 0.85, P_{frac} = 0.4).

Table S3

Parameter	Value	Source
$\left({}^{180}Hf/_{184}W\right)_{CHUR}$	1.35 ± 0.11	Kleine & Walker (2017)
$t_{1/2}$ of ^{182}Hf	8.9 ± 0.1 Myr	Kleine & Walker (2017)
t_{CAI}	4.567 Ga	MacPherson (2014)
$\left({}^{182}Hf/_{180}Hf\right)_{inital}$	$(1.018 \pm 0.043) \times 10^{-4}$	Kruijer et al. (2014)
$\left({}^{182}W/_{184}W\right)_{inital}$	0.865 ± 0.001	Kruijer et al. (2014)
$\left({}^{184}W/_{W}\right)_{modern}$	0.3064 ± 0.0002	IUPAC (2003)
$\left({}^{180}Hf/_{Hf}\right)_{modern}$	0.3508 ± 0.0016	IUPAC (2003)
Martian mantle $f^{Hf/W}$	2.0 ± 0.4	Kleine & Walker (2017)
Martian mantle ε_{182W} (relative to BSE)	0.37 ± 0.04	Kruijer et al. (2017)
CHUR ε_{182W} (relative to BSE)	-1.9 ± 0.1	Kleine & Walker (2017)

Values used for the Hf–W isotopic calculations. Formulations of ε_{182W} and $f^{Hf/W}$ are given in Equations 1 and 2, respectively. In Figures 3, 5, S2, and S3, we compare our analogs to ε_{182W} of the Martian mantle relative to CHUR (2.27 ± 0.14), which is equal to the difference between the Martian mantle ε_{182W} and CHUR ε_{182W} listed here.

Supplementary References

International Union of Pure and Applied Chemistry. (2003). ATOMIC WEIGHTS OF THE ELEMENTS: REVIEW 2000. *Pure and Applied Chemistry*, *75*(6), 683–800.

Jacobsen, S. B. (2005). THE Hf-W ISOTOPIC SYSTEM AND THE ORIGIN OF THE EARTH AND MOON. *Annual. Reviews in Earth and Planetary Sciences*, *33*, 531–70.

Kleine, T., & Walker, R. J. (2017). Tungsten Isotopes in Planets. *Annual Review of Earth and Planetary Sciences*, *45*(1), 389–417.

Kruijer, T. S., Kleine, T., Borg, L. E., Brennecka, G. A., Irving, A. J., Bischoff, A., & Agee, C. B. (2017). The early differentiation of Mars inferred from Hf–W chronometry. *Earth and Planetary Science Letters*, *474*, 345–354.

Kruijer, T. S., Kleine, T., Fischer-Gödde, M., Burkhardt, C., & Wieler, R. (2014). Nucleosynthetic W isotope anomalies and the Hf-W chronometry of Ca-Al-rich inclusions. *Earth and Planetary Science Letters*, *403*, 317–327.

MacPherson, G. J. (2014). Calcium-aluminum-rich inclusions in chondritic meteorites. *Meteorites and Cosmochemical Processes*, 139–179.

Morishima, R., Golabek, G. J., & Samuel, H. (2013). N-body simulations of oligarchic growth of Mars: Implications for Hf-W chronology. *Earth and Planetary Science Letters*, *366*, 6–16.

Nimmo, F., & Kleine, T. (2007). How rapidly did Mars accrete? Uncertainties in the Hf–W timing of core formation. *Icarus*, *191*(2), 497–504.

Palme, H., & O'Neill, H. S. C. (2014). Cosmochemical Estimates of Mantle Composition. In *Treatise on Geochemistry* (2nd ed., pp. 1–39).